Kinetics and Mechanism of Degradation and Tautomerization of Cefotetan in Aqueous Solution

Akira KOSHIRO,*[,a] Toshio FUJITA,[a] Yukiko HARIMA,[a] Kunihiko FUKAI[a] and Fumio YONEDA[b]

The Department of Pharmacy, Yamaguchi University Hospital,[a] 1144, Kogushi, Ube 755, Japan and the Faculty of Pharmaceutical Sciences, Kyoto University,[b] Shimoadachi-cho, Sakyoku, Kyoto 606, Japan. *Received July 11, 1988*

The kinetics of the degradation and tautomerization of cefotetan in aqueous solution was studied at 25 °C and ionic strength 0.6 over the pH range of 2.0—12.0. The degradation rates of cefotetan and its tautomer were found to be identical and the rate law reflected the spontaneous hydrolysis of each molecular species and the hydroxide ion-catalyzed hydrolysis of the dianionic species. The tautomerization was remarkable especially in the alkaline region and the equilibrium of the tautomerization shifted toward the tautomer as the hydroxide ion concentration was increased. Divalent metal ions were found to catalyze the tautomerization by chelation. Electron transfer triggered by the attack of hydroxide ion at the amide of the 1,3-dithiethane moiety and electron withdrawal by hydronium ion from the nitrogen atom on the isothiazole ring of the anion intermediate formed from the tautomer by hydroxide ion were proposed as the mechanisms of the forward and reverse tautomerizations, respectively. The latter reaction is considered to be accompanied with epimerization. The apparent activation energies of the degradation at pH 3.0, 7.0 and 9.0 and those of the forward and reverse tautomerizations at pH 9.0 were 23.3, 22.9, 31.4, 35.5 and 24.4 kcal mol^{-1}, respectively.

Keywords kinetics; antibiotic; cefotetan; cephem; hydrolysis; tautomerization; epimerization; beta-lactam; cephamycin

Cefotetan (**1** in Chart 1) is a cephamycin antibiotic, which was developed by Iwanami *et al.*[1] Cefotetan is an antibiotic for parenteral use. Therefore, the prediction of the stability in an intravenous admixture is important, and kinetic information on the stability is essential. In addition to hydrolysis, the 1,3-dithiethane side chain of cefotetan tautomerizes to form an isothiazole ring (**2** in Chart 1) in aqueous solution, especially in the alkaline region.[1] The epimerization at the asymmetric α-carbon of the benzyl side chains of cefsulodin[2,3] and latamoxef[4,5] are other examples of isomerization of β-lactam antibiotics leading to a decrease of the potency. On the other hand, the tautomer of cefotetan has been reported to have an antimicrobial potency almost equivalent to that of cefotetan.[6] However, the pharmacokinetic behaviors of both isomers may differ from each other as well as from the epimers[7] of cefotetan because of the asymmetric carbon at the dithiethane ring. So, they may not be equivalent from a clinical standpoint. Benzodiazepines are another type of drugs which show a similar reversible reaction in acidic media.[8—11] Various amounts of the tautomer have been detected in urine after dosing of cefotetan to various experimental animals[12] and human[13]; the amount was considered to depend on the urinary concentration of Mg^{2+} and the pH.

In the present study, the kinetics of the degradation and tautomerization of cefotetan and its tautomer in aqueous solution was studied for the purpose of prediction of the stability in an intravenous dosage form and admixtures. In addition, the mechanism of the tautomerization and the interaction with amines were studied briefly.

Experimental

Instruments The high performance liquid chromatography (HPLC) system consisted of a model LC-3A liquid chromatograph (Shimadzu Manufacturing CO., Ltd., Kyoto, Japan), μBondapak C_{18} column (3.9 mm × 30 cm i.d., Water Associates, Milford, MA) and a UVIDEC-100 variable-wavelength detector (Japan Spectrophotometric Co., Ltd., Tokyo, Japan). The output signal from the detector was collected by a model C-R2AX Chromatopac (Shimadzu Manufacturing Co., Ltd.). The thermo-regulators used were model MIR 150 (Sanyo Scientific Industries Ltd., Chiba, Japan) and model F3-K (Haake, Karlsruhe, West Germany) incubators. pH was measured using a model RAT-11S recording autotitrator (Hiranuma Sangyo Co., Ltd., Tokyo, Japan). Kinetic data were analyzed using an ACOS-850 digital computer (Nippon Electric Co., Ltd., Tokyo, Japan).

Materials Authentic samples of cefotetan and its tautomer were generously supplied by the manufacturer (Yamanouchi Pharmaceutical Co., Ltd., Tokyo, Japan) and were used without further purification. Disodium cefotetan for injection was used for the kinetic studies. The other reagents were all of reagent grade (Nakarai Chemicals Ltd., Kyoto, Japan). Buffer solutions used were as follows: pH 2.0—4.0 (0.05—0.2 M disodium citrate–0.05—0.2 N HCl); pH 5.0 (0.05—0.2 M sodium acetate–acetic acid); pH 6.0 and 7.0 (0.05—0.2 M dihydrogen potassium phosphate–hydrogen disodium phosphate); 8.0 and 9.0 (0.05—0.2 M disodium tetraborate–0.05—0.2 N HCl); pH 10.0 (0.05—0.2 M disodium tetraborate–0.05—0.2 M sodium hydroxide); pH 10.75 (0.05—0.2 M sodium carbonate–sodium hydrogen carbonate); pH 11.0—12.0 (0.05—0.2 M hydrogen disodium phosphate–0.05—0.2 M sodium hydroxide). The ionic strength of all buffer solutions was adjusted to 0.6 with KCl.

Kinetic Measurements Disodium cefotetan (3 mg) was dissolved in 10 ml of a buffer solution preequilibrated to a desired temperature so that the final concentration was 4.84×10^{-4} M. Alternatively, 100 μ aliquots of 4.84×10^{-2} M cefotetan aqueous solution were spiked into 10 ml of the buffers to make reaction solutions. The mixtures were incubated at 25 ± 0.05 °C. The reaction was also carried out at 37 and 45 °C for the determination of the apparent activation energies of the degradation and tautomerization. The residual amounts of cefotetan and the tautomer were determined at appropriate time intervals by HPLC. At pH values above 9.0, aliquots of the sample solutions withdrawn at appropriate time intervals were neutralized (pH 6.3—7.0) by adding appropriate amounts of 1.0—2.5 N HCl and frozen until analysis.

Effects of Divalent Metal Ions Various concentrations of divalent metal ions (1.25—5 times the concentration of cefotetan) were added to the mixtures (pH 8.0, 0.2 M tetraborate–0.2 M HCl and ionic strength 0.6 with KCl) and the mixtures were assayed as mentioned above.

Effects of Redox Reagents and Amines Ten-fold molar concentrations of redox reagents (H_2O_2, $HClO_4$, $Na_2S_2O_4$, HCHO, *etc.*) and amines (various alkylamines, imidazole, hydrazine, amino acids, *etc.*) were incubated with 4.84×10^{-4} M cefotetan at pH 9.0 (0.2 M sodium tetraborate–0.2 N HCl) and 25 °C. The pHs of these reaction solutions were readjusted with trace amounts of 2 N NaOH or HCl. The residual cefotetan and tautomer were also assayed.

Assay Procedure Fifty microliters of the mixture and 50 μl of the internal standard solution (8.33×10^{-4} M tegafur) were mixed and 5 μl of the resulting mixture was injected into a chromatograph. The flow rate of the mobile phase (0.1 M NaH_2PO_4 : CH_3CN : CH_3OH : CH_3CO_2H (17 : 1 : 1 : 1)[14]), was 1.0 ml/min. The peaks were detected at 260 nm and quantitation was done by comparison with standard solutions of the authentic samples of cefotetan and the tautomer in 1% phosphate buffer, pH 7.0.

Results and Discussion

Determination of Cefotetan and the Tautomer Figure 1

shows a typical chromatogram of a mixture of cefotetan, the tautomer and tegafur as an internal standard. Both the area and peak height ratios gave linear calibration graphs. The correlation coefficients of the regression lines for both compounds were 0.9999. Reaction during passage through the analytical column was confirmed to be negligible because pure cefotetan and the tautomer, (the latter was obtained in reaction solution of pH 12.0) each gave only a single peak.

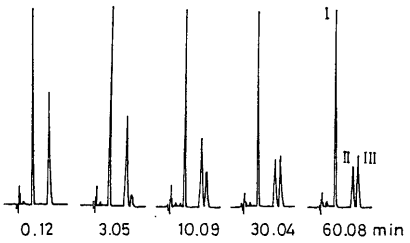

Fig. 1. Chromatograms Obtained during Incubation at pH 10.0, 25 °C and Ionic Strength 0.6

I, tegafur as I.S. (6.70 min); II, cefotetan (10.6 min); III, tautomer (11.7 min).

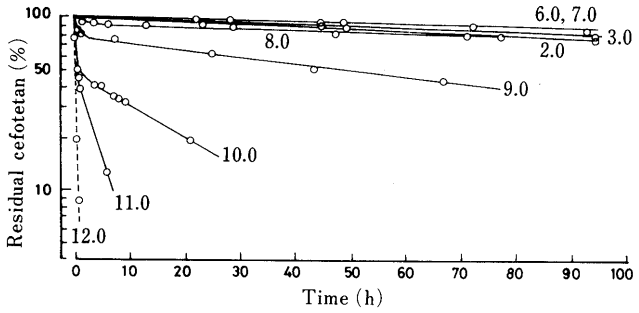

Fig. 2. Time Courses of Decline of Cefotetan in Various Buffer Solutions at 25 °C and Ionic Strength 0.6

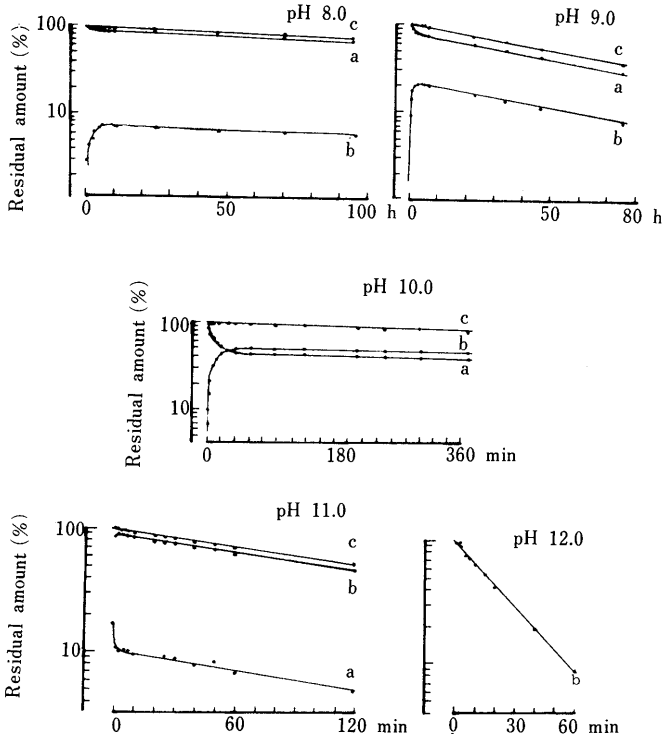

Fig. 3. Time Courses of Declines of Cefotetan (a), the Tautomer (b) and the Sum of Them (c) at pH 8.0—12.0[a] and 25 °C

a) The buffers are those of the highest concentrations in Figs. 4 and 6. Solid lines are computer-generated time courses.

Time Courses of Cefotetan and the Tautomer in Buffer Solutions Figure 1 also shows representative chromatograms of cefotetan and the tautomer during incubation. Figure 2 shows the time courses of cefotetan at various pHs and 25 °C. Rapid biexponential decreases of cefotetan occurred at pH 8—11, indicating rapid formation of the tautomer at the initial phase followed by equilibration as depicted in the chromatograms of Fig. 1. Together with the time courses of cefotetan, those of the tautomer in various buffer solutions are shown in Fig. 3. The formation of the tautomer was observed to various extents over the whole pH range studied. This tautomerization was especially marked in the alkaline region but was minimal in the acidic region. As is clear from Fig. 3, the declines of cefotetan and the tautomer were almost parallel after equilibration in all cases. The sum of cefotetan and the tautomer decreased at the same rate as those of each component, post-equilibrium. Unlike each component, the decline of the sum of them seemed to obey pseudo-first-order kinetics during the whole incubation period. At pH 12.0, only the decline of the tautomer was measured because all of the cefotetan was immediately converted to the tautomer on dissolving.

Construction of the Model for the Reactions of Cefotetan in Aqueous Solution Considering the time courses of cefotetan, the tautomer and the sum of them (Fig. 3), Chart 1 is proposed as a probable model for the reactions of cefotetan in aqueous solution. Using the Laplace transformation technique, the equation which describe the time courses of cefotetan (C_t), the tautomer (T_t) and the sum of them (C_t+T_t) were derived as:

$$C_t=\frac{(k_2^-+k_3-\alpha)C_0+k_2^-T_0}{\beta-\alpha}e^{-\alpha t}+\frac{(k_2^-+k_3-\beta)C_0+k_2^-T_0}{\alpha-\beta}e^{-\beta t} \quad (1)$$

$$T_t=\frac{(k_2^++k_1-\alpha)T_0+k_2^+C_0}{\beta-\alpha}e^{-\alpha t}+\frac{(k_2^++k_1-\beta)T_0+k_2^+C_0}{\alpha-\beta}e^{-\beta t} \quad (2)$$

$$C_t+T_t=\frac{(k_2^++k_2^--\alpha)(T_0+C_0)+k_3C_0+k_1T_0}{\beta-\alpha}e^{-\alpha t}+\frac{(k_2^++k_2^--\beta)(T_0+C_0)+k_3C_0+k_1T_0}{\alpha-\beta}e^{-\beta t} \quad (3)$$

where

$$\alpha=0.5[K+(K^2-4(k_1k_3+k_1k_2^-+k_3k_2^+))^{1/2}]$$

$$\beta=0.5[K-(K^2-4(k_1k_3+k_1k_2^-+k_3k_2^+))^{1/2}]$$

$$K=k_1+k_3+k_2^++k_2^-$$

and k_1 and k_3 are the degradation rate constants of cefotetan and the tautomer, respectively; k_2^+ and k_2^- are the forward and reverse tautomerization rate constants, respectively; C_0 and T_0 are the initial concentrations of cefotetan and the tautomer, respectively.

In the case of $k_1=k_3$, Eqs. 1—3 are reduced to Eqs. 4—6:

$$C_t=\frac{1}{k_2^++k_2^-}[k_2^-(C_0+T_0)e^{-k_1t}+(k_2^+C_0-k_2^-T_0)e^{-(k_1+k_2^++k_2^-)t}] \quad (4)$$

$$T_t=\frac{1}{k_2^++k_2^-}[k_2^+(C_0+T_0)e^{-k_1t}+(k_2^-T_0-k_2^+C_0)e^{-(k_1+k_2^++k_2^-)t}] \quad (5)$$

$$C_t+T_t=(C_0+T_0)e^{-k_1t} \quad (6)$$

If k_1 is not equal to k_3, the time courses of decline of C_t+T_t

should show a biphasic pattern as represented by Eq. 3. But all of the data seemed to be monoexponential, as shown in Fig. 3. In all cases, C_t+T_t declined monoexponentially. This is evidence that k_1 is equal to k_3. In the case of k_2^+ and/or $k_2^- \gg k_1$ or k_3, however, one cannot detect the α phase in Eq. 3 and further evidence is necessary to reach a definite conclusion. On analysis of these data by the nonlinear least-squares method using the program "MULTI,"[15] the AIC value, the Akaike's information criteria,[16] is useful for evaluation of curve fitting of the model. When analyzed according to Eqs. 4—6, much smaller AIC values were obtained than those obtained on analysis according to Eqs. 1—3. This indicates that Eqs. 4—6 are sufficient to describe the behavior of cefotetan in aqueous solution. Furthermore, it is known that the effect of a side chain at C_7 on the stability of the β-lactam moiety of β-lactam antibiotics is small compared to that of a side chain at C_3,[17-19] except for aminobenzyl or oxime substituents, which show intramolecular nucleophilic reaction with the β-lactam ring and steric hindrance, respectively.

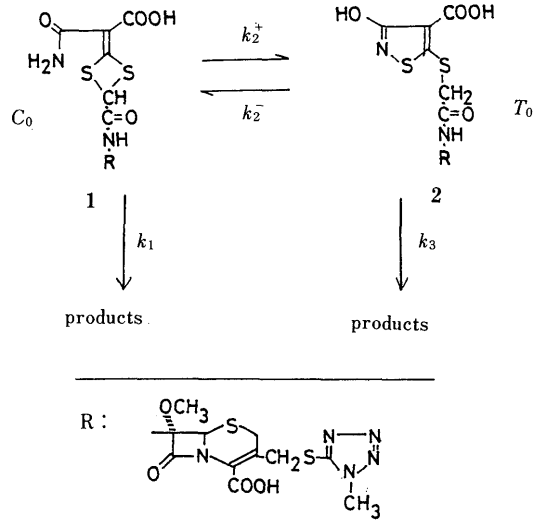

Chart 1. Model of the Reactions of Cefotetan in Aqueous Solution

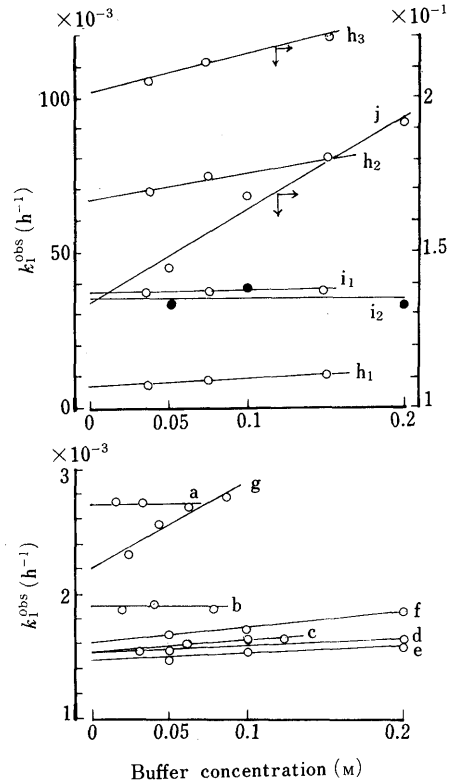

Fig. 4. Observed Degradation Rate Constants at Various pHs and Buffer Concentrations (Ionic Strength 0.6)

a, pH 2.0 (25 °C); b, pH 3.0 (25 °C); c, pH 4.0 (25 °C); d, pH 5.0 (25 °C); e, pH 6.0 (25 °C); f, pH 7.0 (25 °C); g, pH 8.0 (25 °C); h_1, pH 9.0 (25 °C); h_2, pH 9.0 (37 °C); h_3, pH 9.0 (45 °C); i_1, pH 10.0 (25 °C, borate buffer); i_2, pH 10.0 (25 °C, carbonate buffer); j, pH 10.75 (25 °C).

From the above considerations, we analyzed the data according to Eqs. 4—6 using the MULTI program[15] with weightings of 1 at pH 9.0—12.0 and C_t^{-1} below pH 8.0.

pH-Rate Profile of the Degradation of Cefotetan and the Tautomer The observed degradation rate constants, k_1^{obs}s, under various reaction conditions are shown in Fig. 4. When the effects of the buffer components on the degradation of cefotetan and the tautomer were observed as in Fig. 4, k_1 values were obtained as the intercepts of the plots. In the case where the effect of buffer components was uncertain as experienced at pHs 2.0, 3.0 and 10.0 (carbonate buffer), k_1 values were obtained as the averages. The pH-rate profile for k_1 is shown in Fig. 5. Cefotetan has two carboxyl groups, one on the cephem skeleton (pK_{a1} 2.58) and the other on the 1,3-dithiethane side chain (pK_{a2} 3.18). It seems that Eq. 7 holds as a rate law, reflecting the water-catalyzed hydrolysis of each molecular species and the hydroxide ion-catalyzed hydrolysis of the dianion as the same fashion in the cases of other β-lactam antibiotics.[20,21]

$$k_1=\frac{1}{K_{a_1}K_{a_2}+K_{a_1}a_{H^+}+a_{H^+}{}^2}\times(k_{AH2}a_{H^+}{}^2+k_{AH}K_{a_1}a_{H^+}+k_AK_{a_1}K_{a_2}+k_{OH}K_{a_1}K_{a_2}a_{OH^-}) \quad (7)$$

where k_{AH2}, k_{AH}, k_A and k_{OH} are the microscopic rate constants for the water-catalyzed hydrolysis of undissociated acid, monoanion, and dianion and hydroxide ion catalyzed hydrolysis of dianion, respectively. The k_1 values at pH 2.0—10.75 were analyzed according to Eq. 7 by using the nonlinear least-squares method program "MULTI"[15] with a weighting of data k_1^{-2}.The following values were obtained: 3.05×10^{-3} h^{-1} for k_{AH2}, 1.59×10^{-3} h^{-1} for k_{AH},

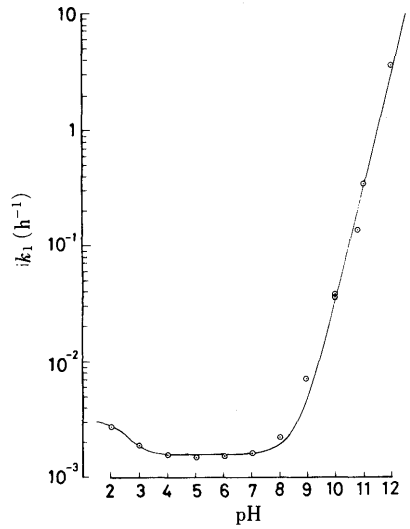

Fig. 5. pH-Rate Profile of the Degradation of Cefotetan and the Tautomer at 25 °C and Ionic Strength 0.6

The solid line is a computer generated pH-rate profile using Eq. 7.

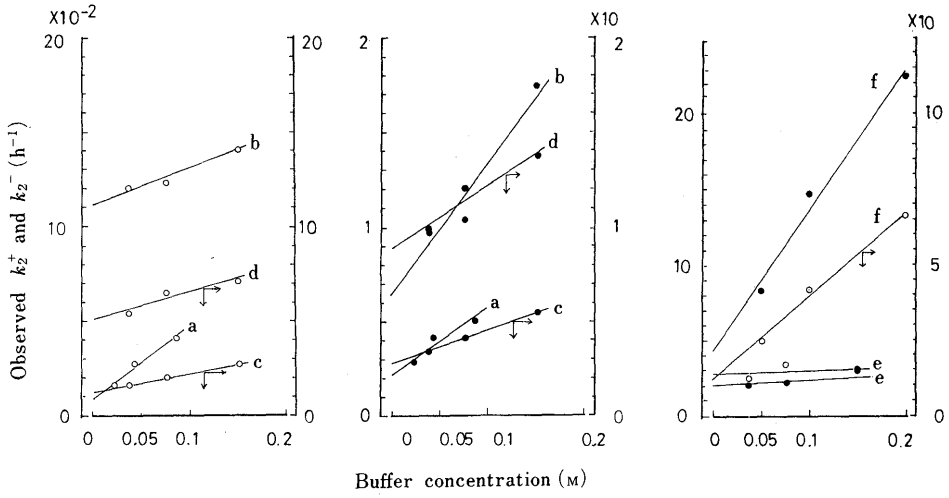

Fig. 6. Observed Forward and Reverse Tautomerization Rate Constants at Various pHs and Buffer Concentrations

○, k_2^+; ●, k_2^-; a, pH 8.0 (25 °C); b, pH 9.0 (25 °C); c, pH 9.0 (37 °C); d, pH 9.0 (45 °C); e, pH 10.0 (25 °C); f, pH 10.75 (25 °C).

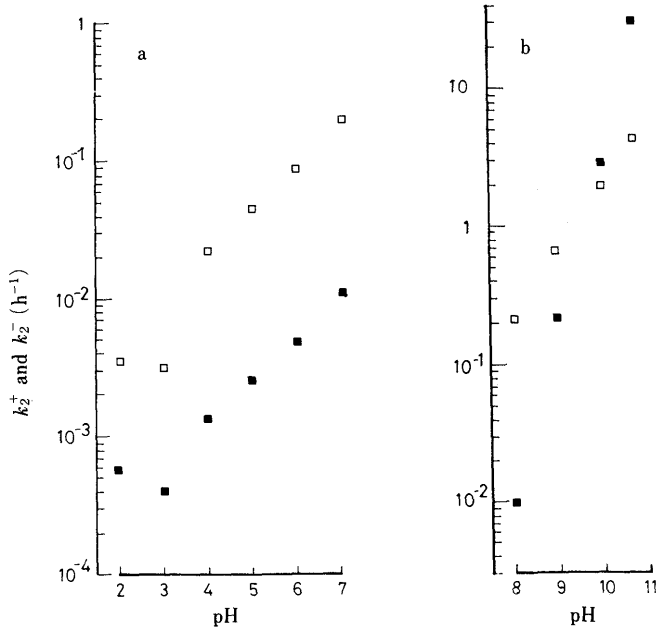

Fig. 7. pH-Rate Profiles of Forward and Reverse Tautomerization Rate Constants at 25 °C and Ionic Strength 0.6

■, k_2^+; □, k_2^-.

$1.60 \times 10^{-3}\,h^{-1}$ for k_A, $3.11 \times 10^2\,h^{-1}\,M^{-1}$ for k_{OH}. The solid line in Fig. 5 is a computer generated pH-rate profile using these values and Eq. 7.

The Tautomerization of Cefotetan and the Tautomer The observed forward and reverse tautomerization rate constants are given in Fig. 6. As shown in Fig. 6, the tautomerization rate was also affected by the buffer components, such as tetraborate and carbonate. General bases thus catalyze the tautomerization. The k_2^+ and k_2^- were obtained by extrapolation. Clear buffer effects on the tautomerization reaction could not be detected in the neutral and acidic regions. Therefore, the k_2^+ and k_2^- in these pH regions were obtained as averages. pH-Rate profiles of the tautomerization reaction thus obtained are given in Fig. 7. As is clear from Fig. 7b, hydroxide ion is a predominant catalyst for the tautomerization. The forward tautomerization rate was affected more than the reverse tautomerization rate. But the values of reverse tautomerization rate constant were much higher than those of the forward tautomerization rate constant below pH 9.0, indicating that cefotetan is the dominant form at neutral pH. In the neutral to acidic region (Fig. 7a), however, the tautomerization rate is slow, although the equilibration constants are 0.054—0.17, which means that the ultimate predominant form is cefotetan. This is significant from a clinical standpoint. For example, if an intravenous admixture of cefotetan in which tautomerization has occurred is

Table I. Effects of Redox Reagents on the Tautomerization and Degradation of Cefotetan at pH 9.0, 25 °C and Ionic Stength 0.6

Reagent	$k_1 \times 10^{-1}$ (h^{-1})	$k_2^+ \times 10$ (h^{-1})	k_2^- (h^{-1})	k_2^+/k_2^-
None[a)]	1.15	3.75	1.55	0.242
Sodium dithionite	1.51	5.40	1.84	0.293
Sodium bisulfite	1.77	5.28	1.61	0.327
Hydrogen peroxide	13.7	5.87	1.81	0.324
Perchloric acid	1.25	6.01	1.88	0.320
Formaldehyde	20.7	5.82	1.83	0.318

a) The concentration of the buffer was 0.131 M and the concentrations of all reagents and disodium cefotetan were 4.84×10^{-3} and 4.84×10^{-4} M, respectively.

Table II. Effects of Divalent Metal Ions on the Tautomerization and Degradation of Cefotetan at pH 8.0 and Ionic Strength 0.6

Divalent metal ion	Conc. (M)	$k_1 \times 10^3$ (h^{-1})	$k_2^+ \times 10^2$ (h^{-1})	$k_2^- \times 10$ (h^{-1})	k_2^+/k_2^-
None[a)]	—	3.19	4.11	5.07	0.081
Mg^{2+}	2.42×10^{-3}	2.14	5.66	1.72	0.329
	1.21×10^{-3}	2.31	2.81	1.93	0.146
Ni^{2+}	2.42×10^{-3}	20.5	41.6	1.02	4.06
	1.21×10^{-3}	37.1	14.3	1.48	0.969
	6.05×10^{-4}	27.7	15.5	1.03	1.51
Mn^{2+}	2.42×10^{-3}	4.79	10.1	1.50	0.670
	1.21×10^{-3}	2.77	3.31	1.02	0.324
Co^{2+}	2.42×10^{-3}	10.9	18.1	0.697	2.59
	1.21×10^{-3}	5.55	8.07	0.921	0.877
Ni^{2+} +EDTA 2Na	2.42×10^{-3}	8.15	4.93	2.52	0.196

a) Buffer: 0.086 M tetraborate–HCl at 25 °C.

administered, some part of the formed tautomer may remain as tautomer in the body because it will be excreted before reaching the equilibrium point where most of the antibiotic is cefotetan.

Effects of Divalent Metal Ions and Redox Reagents on the Degradation and the Tautomerization of Cefotetan To clarify the mechanism of the tautomerization, interactions with divalent metal ions and redox reagents were studied. In some cases, effects on the degradation were also observed in addition to the effects on the tautomerization. The results are listed in Tables I and II, and each effect is discussed separately below.

a) The Tautomerization and Its Mechanism As shown in Table I, none of the redox reagents caused a remarkable effect on the tautomerization, suggesting no contribution of redox reactions to the tautomerization. On the other hand, the tautomerization rates and the equilibrium constants were remarkably influenced by divalent metal ions (Table II). The forward tautomerization was remarkably accelerated in the presences of divalent metal ions, whereas the reverse tautomerization rates was uniformly depressed. The acceleration of the tautomerization rate was in the order of $Ni^{2+} > Co^{2+} > Mn^{2+}$. The effect of Mg^{2+} was obscure in the present study, although Iwanami and coworkers[1] reported that the catalytic effects on the tautomerization were in the order of $Ni^{2+} > Mg^{2+} > Co^{2+} > Cu^{2+}$ at pH 8.8—8.9 and 25 °C. This suggested that the intensity of catalytic effect of each divalent metal ion may vary with pH. The inhibition of the effect of Ni^{2+} by ethylenediaminetetraacetic acid (EDTA) substantiated that the effect of divalent metal ions is due to chelate formation with cefotetan and the tautomer. The values of the equilibrium constants increased in all cases. Divalent ions thus increased the fraction of the tautomer at equilibrium. In conclusion, the forward tautomerization was catalyzed by general bases, specific base and divalent ions.

From this conclusion, the tautomerization mechanism depicted in Chat 2 is proposed. The hydrogen atom of the amide of the 1,3-dithiethane (**1**) is attacked by bases such as hydroxide ion, and deprotonation may occur as the first step of the forward tautomerization. Consecutive electron transfer as shown in Chart 2 may occur subsequently to cleave the C–S bond of 1,3-dithiethane and form an isothiazole ring (**2**). A divalent metal ion may form a chelate at two sites in the cefotetan molecule. One site involves the carbonyl of the amide and the carboxylate of the 1,3-dithiethane side chain. The other involves the sulfur atom and the carbonyl at the RNHCO– moiety. The former chelation may inhibit the rotation of the amide at the 1,3-dithiethane moiety, thus facilitating the electron transfer to form the N–S bond. The latter chelation may accelerate the electron transfer of the nitrogen atom of the amide of the 1,3-dithiethane by lowering the electron density of the sulfur atom and of the carbonyl of the RCONH– moiety of **1**. This catalytic effect of divalent metal ions, however, was less potent than that of hydroxide ion. This indicates that the most significant step for the forward tautomerization is deprotonation from the nitrogen of the amide on the 1,3-dithiethane side chain.

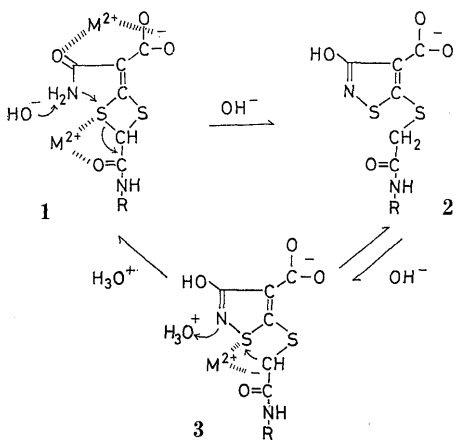

Chart 2. Possible Mechanism of the Tautomerization and the Effect of Divalent Metal Ion on the Tautomerization

The forward and reverse tautomerization rates both decreased with the decrease of pH and were remarkably depressed under acidic conditions, as shown in Fig. 7a. This was further confirmed by the slow reverse formation of cefotetan from the tautomer at this pH region (data not shown). These results strongly suggest that hydroxide ion is also essential in the reverse tautomerization. A probable mechanism is the formation of the anion intermediate (**3**) through deprotonation by hydroxide ion at the active methylene adjacent to the –CONH– moiety of the 7-side chain of the tautomer (**2**). This step is probably rate-limiting. Subsequently, rapid protonation may occur to reform the tautomer. Or, in the presence of sufficient hydronium ion, electron withdrawal from the nitrogen atom in the isothiazole ring of **3** by hydronium ion may occur, and then electron transfer causes the cleavage of the isothiazole ring to form the 1,3-dithiethane structure. Thus, the equilibrium shifts toward cefotetan with decrease of pH, but the reaction rate decrease. In the latter reaction, epimerization may also occur as we previously discussed in connection with the epimerization of cefsulodin.[3]

As indicated in Table II, divalent ion depressed the reverse tautomerization. This may be due to the neutralization of negative charge of the anion intermediate by chelate formation at the site shown in Chart 2, and this may be another mechanism of the catalytic effect of divalent ion on the forward tautomerization.

b) Degradation As shown in Table I, hydrogen peroxide and formaldehyde obviously accelerated the degradation, indicating that the β-lactam moiety is also cleaved by redox reactions. Although other reagents showed little effect on the degradation, sodium bisulfite has been reported to catalyze the degradation of β-lactam antibiotics.[22] The absence of an obvious catalytic effect in the present study is probably due to the pH of the reaction solution, pH 9.0, because the pH-catalytic rate profile of sodium bisulfite is parabolic with a maximum at pH 6.5.[22]

Table III. The Effect of Tromethamine at High Concentration on the Degradation and Tautomerization of Cefotetan at pH 9.0[a] and 25 °C

Conc. of tromethamine (M)	k_1 (h^{-1})	k_2^+ (h^{-1})	k_2^- (h^{-1})
0	0.0115	0.375	1.55
0.05	0.0123	1.11	3.87
0.10	0.0214	1.01	3.74
0.20	0.0157	1.28	4.77

a) Tetraborate buffer (0.131 M).

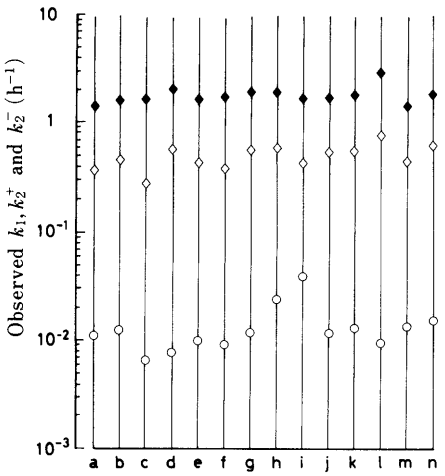

Fig. 8. The Interactions with Amines at pH 9.0, 25 °C and Ionic Strength 0.6

k_1 (○), k_2^+ (◇), k_2^- (◆). The concentrations of cefotetan and amines were 4.84×10^{-4} and 4.84×10^{-3} M, respectively. a, only cefotetan in the buffer (0.131 M tetraborate–HCl); b, ε-aminocaproic acid; c, *n*-butylamine; d, isobutylamine; e, triethylamine; f, ammonia; g, glycerin; h, ethylamine; i, hydrazine; j, Tris; k, imidazole; l, alanine; m, *n*-isopropylamine; n, ethylamine.

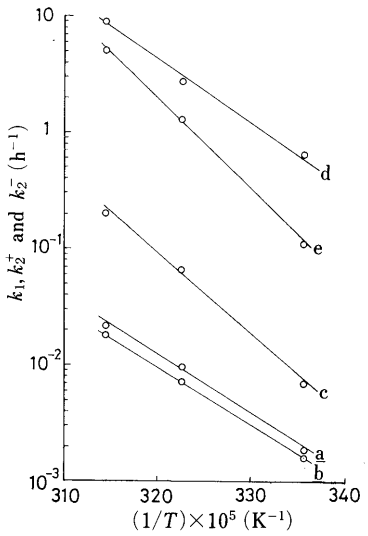

Fig. 9. Arrhenius Plots for the Degradation Rate Constants at pH 3.0, 7.0 and 9.0 and Ionic Strength 0.6

a: k_1, pH 3.0. b: k_1, pH 7.0. c: k_1, pH 9.0. d: k_2^-, pH 9.0. e: k_2^+, pH 9.0.

In addition to the tautomerization, divalent metal ions catalyzed the degradation in the order of $Ni^{2+} \gg Co^{2+} \gg Mn^{2+}$ (Table III). According to Page and coworkers,[23] the intensity of the stimulating effect of hydroxide ion-catalyzed hydrolysis by bivalent metal ions was in the order of $Cu^{2+} > Zn^{2+} > Ni^{2+} > Co^{2+}$ and the stabilization of the tetrahedral intermediate formed by the attack of hydroxide ion on the carbonyl group of the β-lactam by chelation was proposed as the catalytic mechanism. This mechanism seems to explain the current results.

Interaction with Amines Figure 8 shows the degradation rate constants and the tautomerization constants at pH 9.0 and 25 °C in the presence of various amines at ten-fold excess concentration over cefotetan. In the present study, only hydrazine accelerated the degradation of cefotetan, probably by aminolysis. But, the effect of amines on the tautomerization was not marked. In the presence of a high concentration of Tris, 0.05—0.2 M, the tautomerization apparently increased as shown in Table III, indicating that Tris catalyzed the tautomerization as a general base or nucleophile, as did the buffer components shown in Fig. 7.

Effect of Temperature Figure 9 shows Arrhenius plots of the degradation constants at pH 3.0, 7.0 and 9.0 and of the tautomerization at pH 9.0. The apparent activation energies for the degradation were calculated to be 23.3, 22.9 and 31.4 kcal mol^{-1}, respectively. These values indicate that the fraction of the tautomer at equilibrium at pH 9.0 increases as the temperature increases. The activation energies for the degradation and the tautomerization at pH 9.0 were almost equal, substantiating the involvement of hydroxide ion-catalysis in these reactions.

Acknowledgements We thank Professor T. Ban, Department of Pharmacology and Dr. S. Iwamoto, Department of Public Health, Yamaguchi University School of Medicine for advice concerning computation, Miss. A. Nagami and M. Tamura for their help in a part of this work and Yamanouchi Pharmaceutical Industries Ltd. for a generous supply of samples.

References and Notes

1) M. Iwanami, T. Maeda, M. Fujimoto, Y. Nagano, A. Yamazaki, T. Shibanuma, K. Tamazawa and K. Kikuchi, *Chem. Pharm. Bull.*, **28**, 2629 (1980).
2) I. Aoki and K. Konishi and M. Kuwayama, *Iyakuhin Kenkyu*, **9**, 1022 (1978).
3) T. Fujita and A. Koshiro, *Chem. Pharm. Bull.*, **32**, 3651 (1984).
4) R. Weise, N. Wright and P. J. Will, *Review of Infectious Disease*, **4** (Supp.) 564 (1982).
5) N. Hashimoto, T. Tasaki and H. Tanaka, *J. Pharm. Sci.*, **73**, 369 (1984).
6) A. Tachibana, M. Komiya, M. Kikuchi, K. Yano and K. Mashimo, "Current Therapy and Infectious Disease, Proceedings of the 11st International Congress of Chemotherapy and 19th Interscience Conference on Antimicrobial Agents and Chemotherapy," Vol. I, J. P. Nelson and G. Grassi eds., American Society for Microbiology, Washington D.C., 1980, p. 273.
7) F. Kees and H. Grobecker, *J. Chromatogr.*, **305**, 363 (1984).
8) M. Nakano, N. Inotsume, N. Kohri and T. Arita, *Int. J. Pharmaceut.*, **3**, 195 (1979); N. Inotsume and M. Nakano, *J. Pharm. Sci.*, **70**, 1331 (1981).
9) W. H. Hong and D. H. J. Szulcwski, *J. Pharm. Sci.*, **70**, 691 (1981).
10) M. Konishi, K. Hirai and Y. Mori, *J. Pharm. Sci.*, **71**, 1328 (1982).
11) M. Z. Cho, T. A. Schahill and J. B. Jr. Hester, *J. Pharm. Sci.*, **72**, 356 (1983).
12) M. Komiya, Y. Kikuchi, A. Tachibana and K. Yano, *Antimicrob. Agents Chemother.*, **20**, 176 (1981).
13) K. Nakagawa, M. Koyama, A. Tachibana, M. Komiya, Y. Kikuchi and K. Yano, *Antimicrob. Agents Chemother.*, **22**, 935 (1982).
14) T. Sato and K. Yano, Research Laboratory, Yamanouchi Pharmaceutical Co., Ltd., personal communication.
15) K. Yamaoka, T. Tanigawara and T. Uno, *J. Pharmacobio-Dyn.*, **4**, 879 (1981).
16) H. Akaike, *IEEE Trans. Autom. Control*, **19**, 716 (1973). (K. Yamaoka, "Analytical Methods of Pharmacokinetics by Microcomputer," Nankodo, Tokyo, 1984, p. 89).
17) B. Coene, A. Schanck, J. M. Dereppe and M. V. Meorssche, *J. Med. Chem.*, **27**, 694 (1984).
18) J. M. Indelicato, A. Dinner, L. R. Peters and W. W. Wilham, *J. Med. Chem.*, **20**, 961 (1977).
19) M. Narisada, J. Nishikawa, F. Watanabe and Y. Terui, *J. Med. Chem.*, **30**, 514 (1987).
20) E. S. Rattie, J. J. Zimmerman and L. J. Ravin, *J. Pharm. Sci.*, **68**, 1369 (1979).
21) A. Koshiro and T. Fujita, *Yakuzaigaku*, **43**, 36 (1983); T. Fujita, Y. Harima and A. Koshiro, *Chem. Pharm. Bull.*, **31**, 2103 (1983).
22) M. Terao, E. Marui, S. Yonezawa and N. Kawashima, *Yakugaku Zasshi*, **102**, 978 (1980).
23) N. P. Genssmantel, P. Proctor and M. I. Page, *J. Chem. Soc., Perkin Trans. 2*, **1980**, 1725.